ACS APPLIED MATERIALS & INTERFACES

Research Article

www.acsami.org

Self-Running Liquid Metal Drops that Delaminate Metal Films at Record Velocities

Mohammed Mohammed, Rishi Sundaresan, and Michael D. Dickey*

Department of Chemical and Biomolecular Engineering, North Carolina State University, 911 Partners Way, Raleigh, North Carolina 27695, United States

S Supporting Information

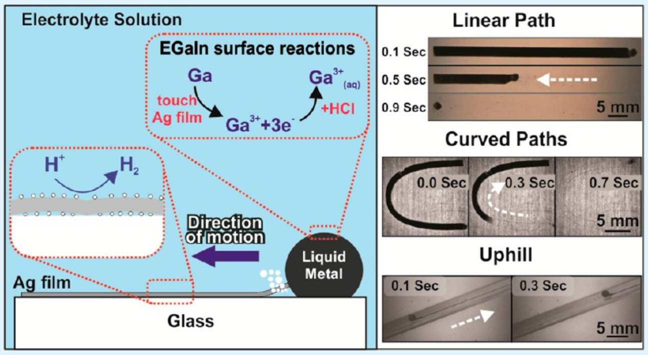

ABSTRACT: This paper describes a new method to spontaneously accelerate droplets of liquid metal (eutectic gallium indium, EGaIn) to extremely fast velocities through a liquid medium and along predefined metallic paths. The droplet wets a thin metal trace (a film ∼100 nm thick, ∼ 1 mm wide) and generates a force that simultaneously delaminates the trace from the substrate (enhanced by spontaneous electrochemical reactions) while accelerating the droplet along the trace. The formation of a surface oxide on EGaIn prevents it from moving, but the use of an acidic medium or application of a reducing bias to the trace continuously removes the oxide skin to enable motion. The trace ultimately provides a sacrificial pathway for the metal and provides a mm-scale mimic to the templates used to guide molecular motors found in biology (e.g., actin filaments). The liquid metal can accelerate along linear, curved and U-shaped traces as well as uphill on surfaces inclined by 30 degrees. The droplets can accelerate through a viscous medium up to 180 mm/sec which is almost double the highest reported speed for self-running liquid metal droplets. The actuation of microscale objects found in nature (e.g., cells, microorganisms) inspires new mechanisms, such as these, to manipulate small objects. Droplets that are metallic may find additional applications in reconfigurable circuits, optics, heat transfer elements, and transient electronic circuits; the paper demonstrates the latter.

KEYWORDS: *liquid metal, EGaIn, self-running, metal films, film delamination, transient electronics*

INTRODUCTION

This paper describes a new method for controlling the motion of droplets of liquid metal along metallic traces while simultaneously delaminating the traces. Controlling the self-motion of liquid droplets has applications in the fields of microfluidics,[1,2] liquid transportation,[3,4] printing,[5] and drug delivery.[6] Nature offers a source of inspiration for new methods to autonomously control the movement of droplets. For example, certain insects and plants survive in desert habitats by manipulating microdroplets of water condensed from fog.[7,8] Likewise, the locomotion of cells and microscopic organisms inspires new methods for controlling the motion of microscale droplets. Here, droplets of liquid metal placed on traces of thin metal films generate forces that simultaneously delaminate the films and accelerate the droplets through a liquid medium at velocities (body length per time) that nearly match the fastest aquatic species known to man. To a first approximation, this new mechanism may be envisioned as analogous to the way humans climb ropes; that is, pulling themselves along a semirigid path that has a cross-sectional area significantly smaller than the human body. Biology also uses "ropes" in the form of microtubules and microfilaments (e.g., actin) across which motor proteins (dynein, kinesin, and myosin) move.[9,10] Although the mechanistic details differ, the work here provides a microscale analog to these molecular scale biological processes through the use of a mechanical template (i.e., the metal trace). This paper describes this new approach for accelerating liquid metal droplets along controlled pathways.

Gradients in surface forces often drive the motion of self-running droplets.[11,12] The gradients may arise from thermocapillarity,[13−16] gradients in chemical species,[17−22] reactive wetting,[23−29] physical surface structures (e.g., asymmetric topography on a surface),[30−33] or using external triggers[34−38] (including voltage[34,39]). In general, these approaches often utilize asymmetric contact angles on both sides of the droplet to induce motion,[40,41] which often requires vibrations to reduce pinning and drag of the droplets.[42,43] Here, the droplets accelerate primarily because of asymmetric forces rather than asymmetric contact angles.

Although most self-running studies focus on aqueous liquids, the self-motion of liquid metals is interesting because these fluids have metallic electrical and optical properties. Liquid metals have larger surface tensions and densities than water; the former is favorable for self-running, while the latter creates

Received: July 30, 2015
Accepted: October 1, 2015
Published: October 1, 2015

ACS Publications © 2015 American Chemical Society

DOI: 10.1021/acsami.5b06978
ACS Appl. Mater. Interfaces 2015, 7, 23163−23171

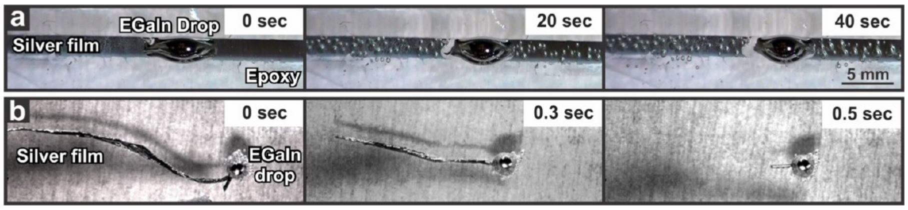

Figure 1. (a) Snapshots of an EGaIn drop contacting a silver film bonded to epoxy in 2 M HCl solution. (b) Snapshots of an EGaIn drop wetting a silver film floating on the surface of 2 M HCl solution. The EGaIn pulls the metal film into the droplet (from left to right), where it presumably dissolves.

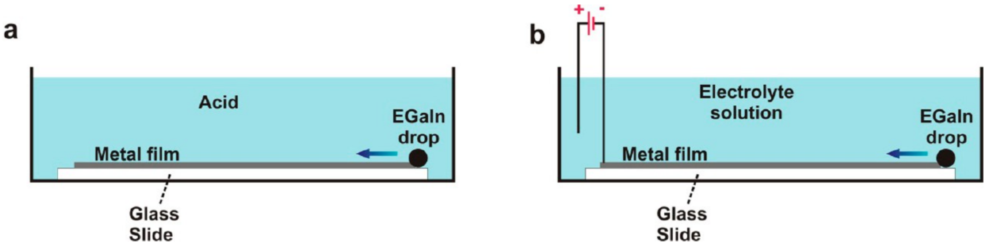

Figure 2. Schematic side view diagrams of EGaIn drops that accelerate over thin metal films. The metal only accelerates in the absence of the surface oxide, which can be removed by (a) acid and (b) electrochemical reduction.

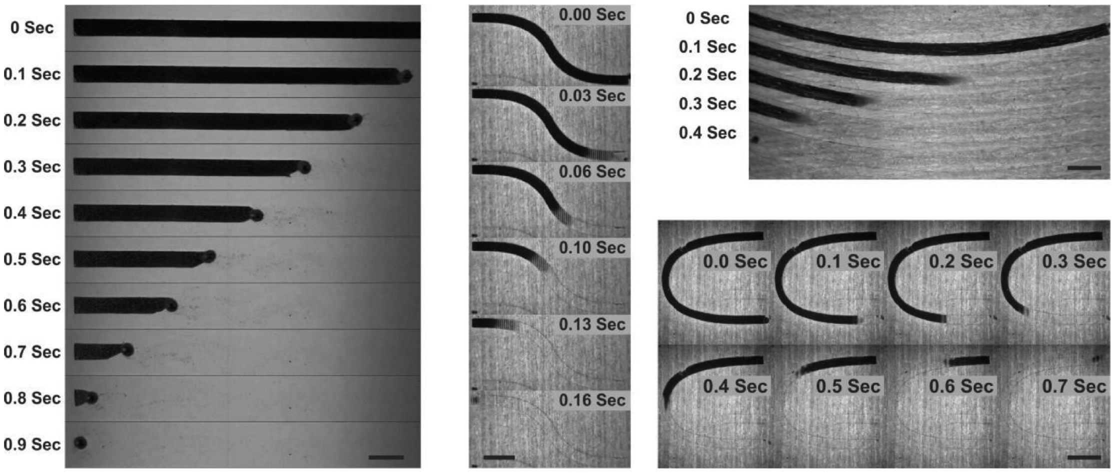

Figure 3. Back-lit, top-down snapshots of EGaIn droplet running on traces of 90 nm of Ag on 10 nm of Au with straight and curved geometries. The glass substrate that supports the metal traces is submerged in 2 M HCl. Scale bar is 5 mm.

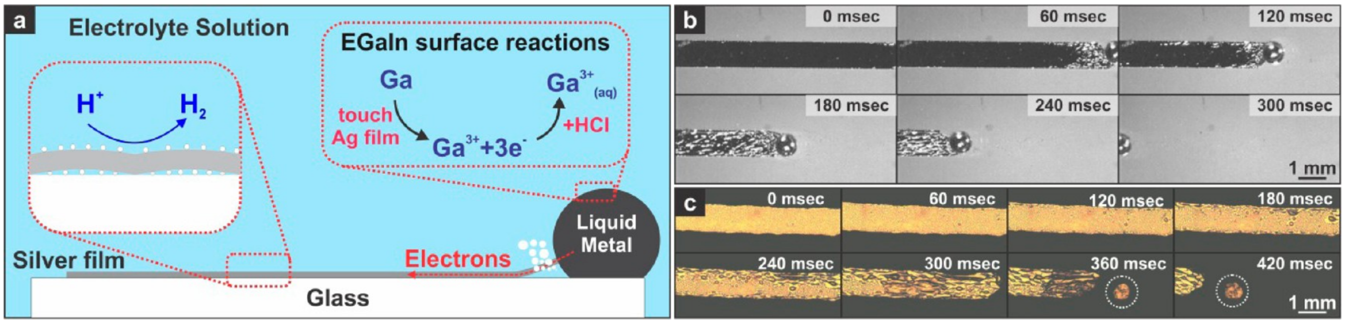

Figure 4. (a) Depiction of an EGaIn drop contacting a Ag/Au layered film on a glass slide showing the electrons migrating from the liquid metal to the film leading to proton reduction and formation of hydrogen bubbles on both sides of the film, (b) Top-down and (c) bottom-up snapshots of a 90 nm silver/10 nm gold film contacted with an EGaIn drop moving right to left in 2 M HCl solution. Dotted circles highlight the EGaIn drop.

inertia that makes it more difficult to accelerate droplets. Liquid metal drops can move over surfaces or in microchannels using electrostatic charges,[44−46] reactions,[47,48] chemical gradients,[49] evaporation of a component from the surface,[50−53] bubble propulsion,[54] or electric fields.[55]

This paper introduces a new mechanism for accelerating liquid metal droplets that delaminate thin metal traces with a speed higher than any reported in literature for liquid metals. The liquid metal drops move spontaneously by wetting, delaminating, and dissolving a thin metal film on a substrate

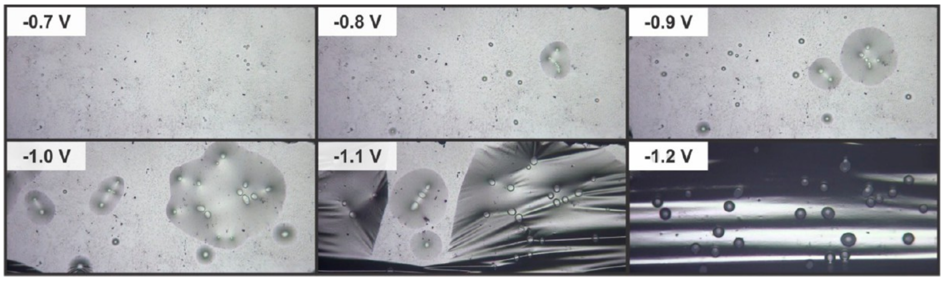

Figure 5. Bottom-up images of 90 nm Ag/10 nm Au trace on a glass slide in 1N NaF solution. The small circles indicate the tiny gas bubble formed at −0.7 V that become more pronounced as the potential becomes more reducing. The bubbles cause the film to delaminate.

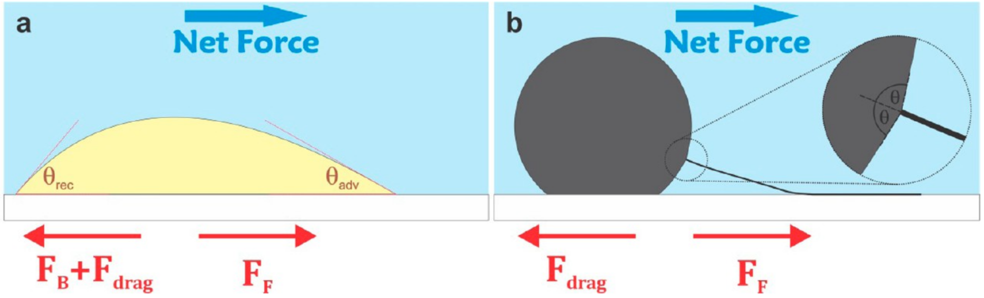

Figure 6. (a) Schematic diagram of the classical profile of a moving drop on a substrate where the drop has two contact angles (advancing and receding angles) with the surface, (b) schematic diagram of the running EGaIn drops where the film delaminates and the two contact angles of the drop with the substrate are approximately the same on both sides of the drop.

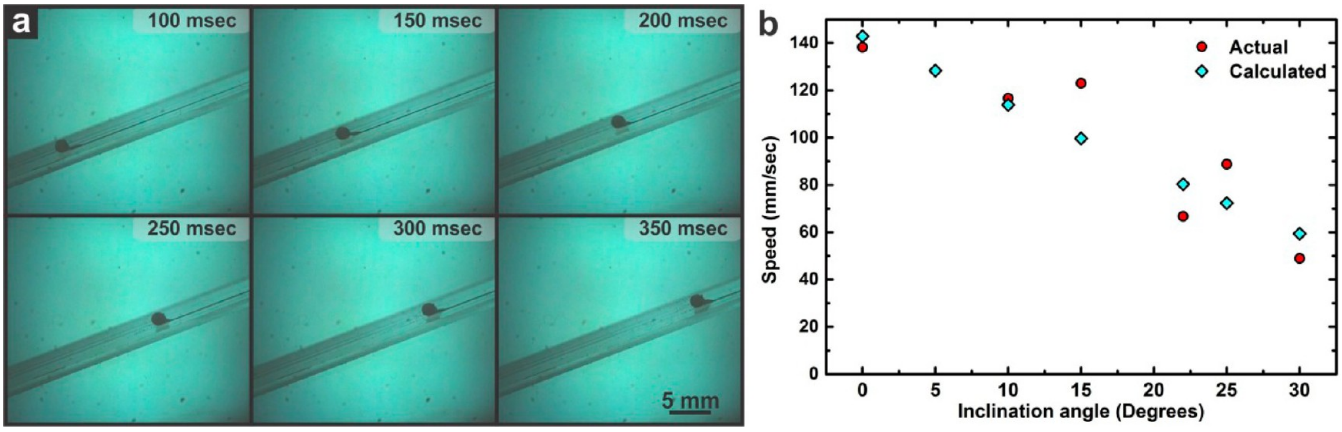

Figure 7. (a) Snapshots of 1 mm EGaIn drop going uphill at 22 degrees inclination angle on a Ag/Au trace patterned on glass, (b) measured and theoretical speed of 0.7 mm diameter EGaIn drop running on 1 mm width Ag/Au trace at different inclination angles.

that serves as a template along which the liquid metal accelerates. We demonstrate and elucidate this new mechanism by which the liquid metal moves.

■ RESULTS AND DISCUSSION

The eutectic alloy of gallium and indium (EGaIn, 75 wt %Ga) is liquid at room temperature (mp = 15 °C)[56] and has low viscosity, high surface tension and high metallic conductivity.[57,58] EGaIn spontaneously forms a thin passivating skin of gallium oxide in the presence of oxygen that allows EGaIn to take nonspherical shapes despite its high surface tension.[59] Even though EGaIn contains indium, the skin consists primarily of gallium oxide because of its reactivity. Acid, base, and electrochemical reduction can remove the skin.[60,61]

To get droplets of EGaIn to accelerate, we take advantage of the high affinity of EGaIn with other metals. For example, EGaIn wets spontaneously smooth In surfaces[62] and liquid Ga wets and eventually dissolves thin Ag films in ambient conditions.[63]

We speculated initially that this wetting property could be harnessed for self-running in a conventional manner. For example, the leading edge of a droplet of liquid metal could wet a film of Ag and pull the droplet toward more Ag. As the droplet moves, it could dissolve the underlying Ag, causing the lagging edge of the drop to assume a large, nonwetting contact angle. The resulting asymmetry would, in principle, propel the droplet in a manner similar to reactive wetting. In reality, EGaIn drops did not run the way we anticipated and its behavior varied dramatically according to the preparation of the Ag film. Figure 1a shows top-down photographs of a drop of EGaIn contacting a silver film on epoxy in 2 M HCl solution. The acid ensures removal of the surface oxide from the droplet of EGaIn. We first deposited the Ag trace on a glass slide and then template stripped it from the slide using epoxy to expose a

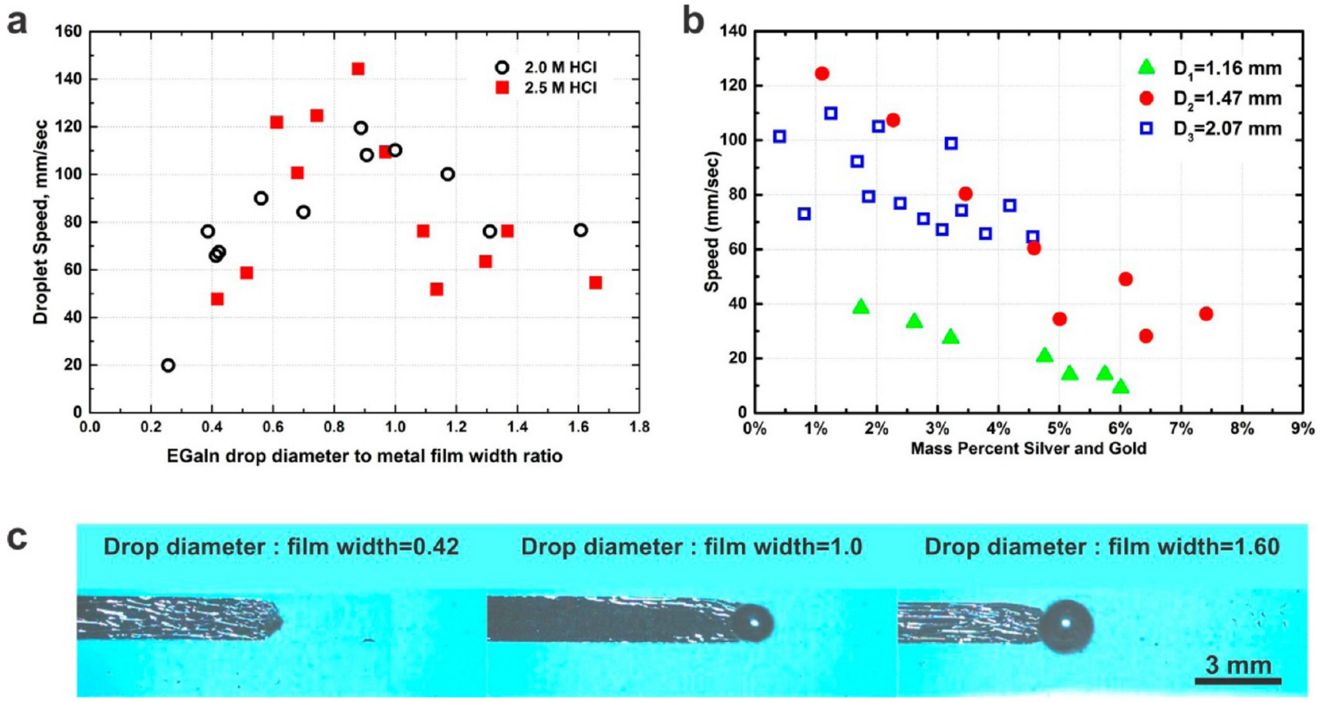

Figure 8. (a) Plot shows the effect of the ratio of drop diameter to metal film width on speed for drops running on Ag/Au. (b) Plot shows the effect of mass percent of Ag and Au in the EGaIn drop on speed for different diameters in 2 M HCl on a 2 mm wide film of Ag/Au. (c) Top-down images of drops having different diameters on 1.5 mm wide Ag/Au film.

Table 1. Comparison between Speeds of Current Self-Running EGaIn Droplets and Other Self-Moving Liquid Metal Droplets in Literature

		maximum speed	
motion induced by	droplet	mm/sec	body length/s
electrostatic actuation[44]	mercury	<1	<1
evaporation of surface species	gallium[51] indium[70]	<1	<1
bubble propulsion[54]	WO_3-coated galinstan marbles	9	9
reaction with other species[48]	Galinstan	50	12.5
electric field[55]	WO_3-coated galinstan marbles	100	50
this work (film delamination)	EGaIn	180	180

pristine Ag surface. The EGaIn wets the Ag film and slowly dissolves it, which is apparent on the left edge of the droplet. The droplet does not accelerate along the Ag, which we attribute to the excellent adhesion between the Ag film and epoxy. Notably, gas bubbles (presumably hydrogen) form on the surface of the silver film a few seconds after the EGaIn drop touches (Video S1).

Figure 1b shows that the liquid metal pulls a free floating film of Ag toward it and consumes the film in less than one second (Video S2). Importantly, the metal droplet does not move significantly, which suggests electrochemical reactions and any resulting electrocapillary phenomena are insufficient to propel the droplet. Instead, wetting between the EGaIn and Ag pulls the film into the droplet. The droplet has significantly more mass than the film (∼100 times heavier), which explains why the film moves rather than the drop.

Figure 1 suggests that EGaIn wets Ag, but self-running will not occur if the Ag film binds strongly to the substrate, nor will it occur if the Ag floats free from the substrate. In contrast, the liquid metal will "sprint" along the metal film if the film and the substrate adhere weakly.

To achieve a weakly bound film, we thermally deposited a thin layer of Au (10 nm) between the Ag (90 nm) and the substrate (glass slides) through stencil masks. Although Ag adheres poorly to most oxide-terminated substrates (e.g., a glass slide), Au has even worse adhesion because it is a noble metal.[64] Relative to the other substrates we used (Kapton, polydimethylsiloxane, poly(methyl methacrylate)), the fastest velocities occurred on glass substrates.

We produced EGaIn drops with desired volumes by molding[65] and contacted them with the metallic traces. The liquid metal only self-sprints in the absence of the oxide layer. The oxide impedes flow and limits contact between the liquid metal and underlying film. Figure 2 shows schematic diagrams of two approaches to remove the oxide and thereby enable self-running. In Figure 2a, acid removes the oxide and in Figure 2b electrochemical reduction removes the oxide. In the latter scenario, the droplet moves only upon application of a reducing potential and stops moving in the absence of potential, thereby providing a mechanism to turn on and off the motion of the droplet.

The shape of the film dictates the path in which the liquid metal drop travels. Figure 3 shows top-down images of different traces that EGaIn self-runs along. EGaIn drops can follow linear paths with velocities up to 180 mm/sec through acidic water, and despite the high inertia of the drops, they can travel on curved and even U-shaped paths (Video S3).

The best self-running occurred with a bilayer film of silver (90 nm) over thin gold (10 nm), which takes advantage of the poor adhesion of gold to glass and the high rate of dissolution of silver in EGaIn. Films of pure Ag also work, but result in

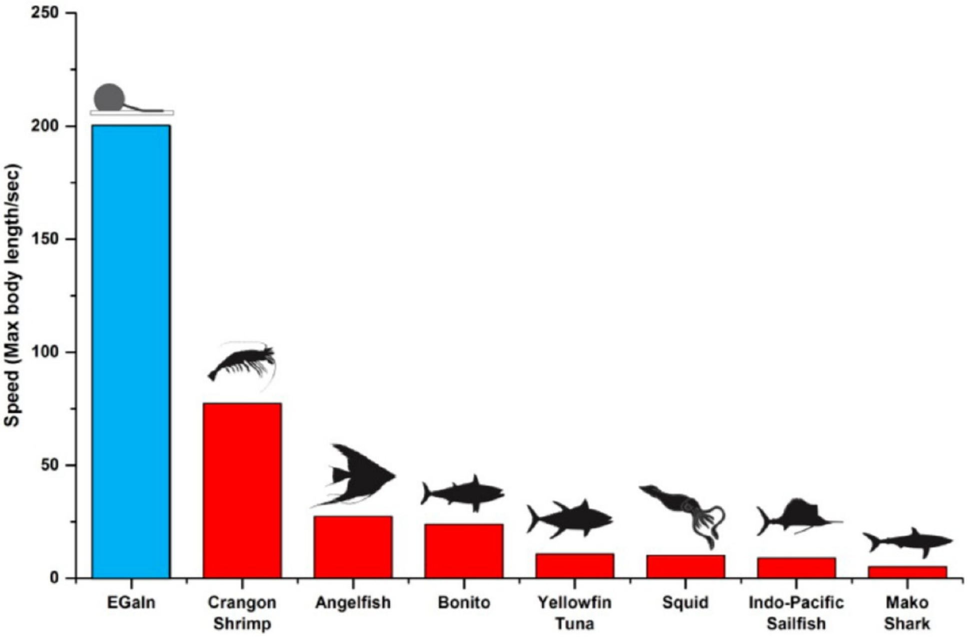

Figure 9. Comparison between the speed of a self-running EGaIn drop and the maximum speeds of the fastest known aqueous creatures in units of body lengths per second. Adapted with kind permission from Spring Science+Business Media.[69]

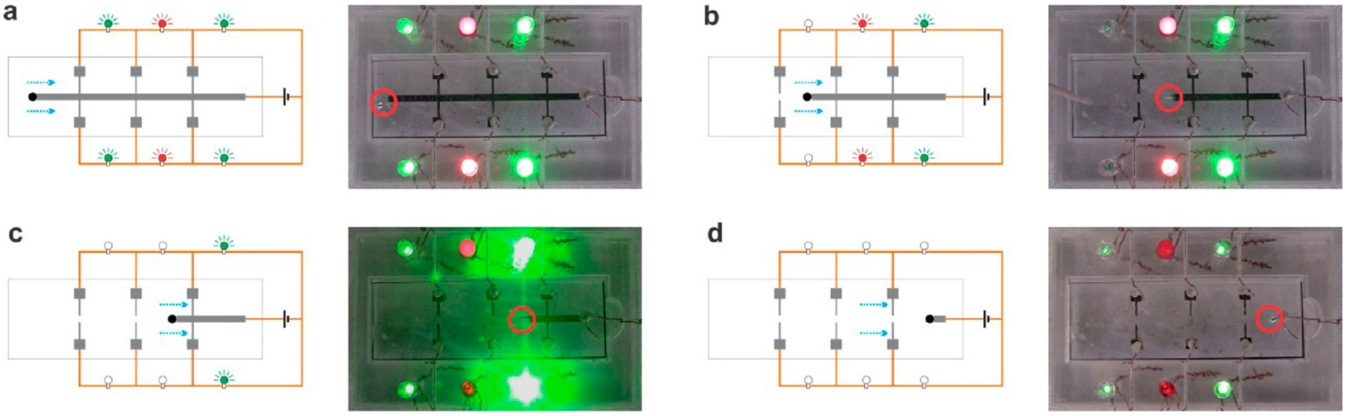

Figure 10. Schematics and photographs of a simple electric circuit spontaneously destroyed by a liquid metal drop that delaminates a solid metal trace. (a) Circuit totally connected, (b) two lamps disconnected, (c) four lamps disconnected, and (d) the whole circuit disconnected. The metal droplet is circled in each photograph.

slower velocities due to the stronger adhesion of Ag to glass relative to Au. Films of pure Au do not work as well as Ag for self-running. Experiments suggest EGaIn dissolves Ag at a faster rate than Au (Figure S2 shows EGaIn "eating" a film of Au over a significantly longer time).

During the experiments reported in Figure 2, we observed that the metal films wrinkled, which facilitates delamination and occurs in every instance of self-running. The bilayer traces wrinkle slightly after immersion in HCl solution; these wrinkles never occurred in the case of pure Au or pure Ag traces (more details in the Supporting Information). The wrinkles became significantly more pronounced when the liquid metal contacts the metal film. We speculated that the liquid metal drop forms an electrochemical cell with the metal film due to the observation of bubbles at the interface between the film and the glass slide. Figure 4a depicts the electrochemical mechanism. The standard potential of silver is higher than that of EGaIn so electrons migrate from EGaIn to the metal film; thus, the EGaIn-Ag film acts as a bipolar electrode. Bipolar electrodes are electrodes that undergo both oxidation and reduction reactions on opposite sides on their surface.[66] Here, oxidation of gallium occurs on the surface of EGaIn and reduction of water occurs on the surface of Ag, which is consistent with the presence of bubbles on the Ag film (cf., Figure 1). In addition, the droplets only self-run in 2−3 M HCl solutions. Although 1 M HCl has a sufficiently low pH to remove the oxide of an isolated drop of EGaIn, the necessity to use >1 M HCl to remove the oxide suggests there is an additional driving force for oxidation, against which the acid must compete (Video S4). Also, the decreased pH favors the reduction of protons to form hydrogen, which is the half reaction that accompanies the oxidation of EGaIn. EGaIn did not run in 1 M NaOH solutions (nor did bubbles form), even though base is known to remove the oxide from an isolated drop of EGaIn. Taken in sum, these observations suggest that acid serves to remove the oxide while simultaneously lowering the reduction potential of water by providing excess protons. To our surprise, these electrochemical reactions occur favorably at the interface between Au and glass (likely due to the higher standard potential of Au relative to Ag), which promotes delamination of the metal film.

Figure 4b presents top-down images of the wrinkles that form when an EGaIn drop contacts a 90 nm Ag film on 10 nm of Au in 2 M HCl solution The bottom-up images in Figure 4c show the formation of tiny bubbles upon initial contact. The bubbles grow and merge to form bigger bubbles that wrinkle and delaminate the film in the region closest to the droplet of EGaIn. The wrinkles are apparent on the entire metal strip, but are most pronounced close to the drop, as shown in Figure 4b and 4c.

It is also possible to generate bubbles by applying a reducing bias to the film without contacting it with EGaIn. A cathodic potential applied to a film of Ag/Au on a glass slide in electrolyte causes the formation of bubbles between the film and glass. Figure 5 shows the formation of the first bubble at −0.7 V (vs Ag/AgCl electrode), more bubbles form as the bias increases until it delaminates completely at −1.2 V. This observation suggests that the bubbles are hydrogen gas that evolves due to water electrolysis according to the equation

$$2H_2O + 2e^- \rightarrow H_2 + 2OH^- \; E = -0.83 \text{ V}$$

Repeating the same experiment on pure Au or pure Ag films forms bubbles on the top surface of the metal film. Bubbles only appear at the bottom interface (i.e., between these pure films and the substrate) when the voltage reaches −1.5 V. Thus, the film stack of Ag/Au increases the formation of bubbles at the bottom interface relative to pure metal films for otherwise identical conditions.

The results presented thus far explain conditions necessary for accelerating droplets of EGaIn, but do not completely explain the forces involved. The classical way by which liquid droplets self-run on a surface depends on asymmetric surface wetting; that is, different contact angles on the two sides of the drop (advancing and receding angles, Figure 6a). The net force acting upon the drop is the difference between the forward and backward forces[13]

$$F_{\text{net}} = F_{\text{F}} - F_{\text{B}} = \gamma(\cos(\theta_{\text{rec}}) - \cos(\theta_{\text{adv}}))w$$

where γ is the surface tension of the moving drop, θ_{rec} and θ_{adv} are the receding and advancing contact angles respectively and w is the width of the drop. This equation neglects the effects of viscous drag since self-running is often done in air.

High speed videos of running drops enable an estimate of the contact angles of the EGaIn drop against the substrate. The advancing and receding angles are nearly identical (149°) and suggests the new propulsion mechanism shown in Figure 6b (Figure S6 shows both angles). The wetting of the drop to the film creates a tensile force on the film. The film comes off the surface at an angle of approximately 20 degrees. The tensile force resolved normal to the substrate delaminates the film and the tensile force resolved parallel to the substrate accelerates the droplet. As a result, the film contacts the droplet at a point elevated relative to the substrate (cf. Figure 6b). This explanation is consistent with the gap between the EGaIn drop and the metal film in the last two bottom-up images in Figure 4c and the delamination that precedes the droplet in Video S5. Importantly, because there is effectively minimal asymmetry in the contact angle between the metal drop and the glass (i.e., $F_{\text{B}} = 0$), the only opposing force to motion is the drag of the droplet as it moves through the electrolyte.

The liquid metal wets the top and bottom of the metal trace, thereby doubling the forward force (F_{F}). The droplet accelerates until the drag force balances the forward force (we neglect friction with the substrate since the droplet barely contacts the substrate). The force balance equation can be written as

$$F_{\text{net}} = F_{\text{F}} - F_{\text{drag}} = 2\gamma\cos(\theta)w - 3\pi\mu D_{\text{P}}v_{\text{drop}}$$

where w is the film width, μ is the liquid medium viscosity, D_{P} is the particle diameter, and v_{drop} is the velocity of the running drop. For the sake of simplicity we used Stoke's law to estimate the drag force. This equation assumes a perfectly spherical drop in a bubble-free fluid at low Re number, which is an oversimplification, but provides a first order estimate of the forces involved. A 1 mm diameter EGaIn drop on a 100 nm thick trace accelerates to ∼13 cm/s, resulting in a drag force of force of ∼1.5 μN. At steady state, we assume $F_{\text{net}} = 0$, which results in a contact angle of 89°. A snapshot from a high speed video estimates this angle to be almost 90° (Figure S6). The large surface tension of the metal enables enormous velocities despite the relatively large contact angle (note: the equilibrium contact angle of EGaIn on Ag is much smaller than reported for this dynamic process).

Despite the high density of EGaIn, the force acting on the drop is enough to rapidly pull the drop uphill on surfaces inclined by angles up to 30 degrees against gravity through a viscous medium (2 M HCl). Figure 7a shows snapshots of an EGaIn drop going uphill on a glass slide tilted by 22° (Video S5). Figure 7b shows the calculated and measured drop speeds with the increase in inclination angle. We calculated the theoretical speed by equating the forward force with the summation of the drag force and the gravitational force $F_{\text{g}} = mg\sin(\phi)$, where ϕ is the inclination angle of the substrate.

Both the ratio of the drop diameter to film width and the amount of film consumed by the liquid metal affect the speed of the droplets. We calculated the speed by recording videos (top-down, bottom-up, or from the side) of the running drops while using computer software to estimate velocity. The results suffer from some noise due to the high speed of the drops and the variability of the adhesion of the films to the substrate, but trends do emerge from the data.

Figure 8a shows the dependence of the drop speed on the ratio of droplet diameter to film width. EGaIn drops with small diameters have small surface areas and volumes which seem to slow down the dissolution of the metal film and therefore the speed (future modeling efforts should consider accounting for the effect of dissolution on speed). The speed increases as the drop diameter increases until it reaches the maximum value at drop diameter to film width ratio of 0.9. Beyond this ratio, the speed decreases because of the increasing mass and drag that requires more force to move. Figure 8c shows top-down images of three drops of different diameters running on 1.5 mm wide film of Ag/Au in 2 M HCl solution (Video S6).

We measured the velocity of individual EGaIn droplets after running sequentially over a known number of metal films. The film dimensions allow calculation of the weight of gold and silver in the EGaIn and hence the final weight percent of gold and silver after "consuming" each line. Drops tend to slow down as the mass percentage of the film increases in the liquid metal. The lowered velocity may be due to the decreased rate of dissolution of Ag and Au. In principle, the Ag and Au could also affect the interfacial tension, although we did not observe significant changes to the wetting between the liquid metal and the film stack during these experiments. Figure 8b shows the reduction of speed of EGaIn drops as the mass percentage of the dissolving metal increases for different drops running over 100 nm films of Ag/Au. EGaIn drops with >20% mass Ag/Au turns to a paste and either run slowly or does not run at all. An EGaIn drop with 1.5 mm diameter needs to run over more than 3 m of 100 nm thick film to reach this weight percent.

To the best of our knowledge, only two systems achieved running speeds for drops that exceed the speed reported in this paper.[32,33] These studies accelerated droplets of water, which has a density six times lower than EGaIn, through air, which has ~50× lower viscous drag than the acid or electrolyte solutions used here. EGaIn drops run on metal films with a speed that almost doubles the maximum reported speed in literature for a liquid metal despite running in a liquid medium. The mechanism is simple and requires no special surface treatment or vacuum conditions. Table 1 summarizes the reported speeds for different liquid metal drops in literature in absolute speed (mm/s) and in units of body lengths per second to give a better means of comparing the speeds of different modes of locomotion. The speed of the EGaIn drops is not only faster than other liquid metal runners, but to the best of our knowledge, is also faster than all swimming creatures in water in units of body lengths per second. The speed of the liquid metal is also higher than speeds of microorganisms that are smaller in size than EGaIn drops such as bacteria and worms; for instance the speed of *C. Elegans* ranges from 0.15 to 1.5 body lengths/s.[67,68] Figure 9 compares the speed of running EGaIn drops to the reported speeds of the fastest swimming creatures known to man.[69]

The use of droplets with metallic properties may provide electrical, physical, and thermal functionality that is not possible with other fluids. We demonstrate one example where we use the self-running EGaIn drops to create self-destructing, transient electronic circuits. As shown in Figure 10, we created a simple circuit to power LEDs. A drop placed in the circuit followed a straight-line path and removed a metal trace from the circuit, sequentially turning off the LEDs. The presence of electrolyte allows the LEDs to operate in a diminished state until the electrolyte evaporates (not shown).

■ SUMMARY

We demonstrated a novel system for self-running liquid metal drops on thin metal traces deposited on glass slides. Liquid metal drops only run in the absence of the surface oxide and on weakly adhered metal films. The liquid metal drop delaminates and consumes the film as it runs. Self-running EGaIn drops can run in straight paths, curved paths and even uphill with angles up to 30 degrees. The speed by which the liquid metal runs is higher than any reported speed in literature for metals despite moving through a viscous liquid medium and exceeds the velocity (body length per time) of the fastest aquatic creatures known to man. Running liquid metal drops have potential applications in fabricating self-destroying electric circuits and more broadly, as a new mechanism to propel microscale objects spontaneously along templated paths to mimic microscale actuation found in nature.

■ ASSOCIATED CONTENT

Ⓢ Supporting Information

The Supporting Information is available free of charge on the ACS Publications website at DOI: 10.1021/acsami.5b06978.

Experiments showing the effect of acid on the wettability of liquid metal on solid metal films; microscope images of a film of 90 nm Ag on 10 nm Au that buckles after contact with 2 M HCl; photograph showing the angles of contact between the liquid metal drop with both the glass substrate and the metal film (PDF)

Video S1 shows a liquid metal drop contacting a silver film bound to epoxy and submerged in 2 M HCl solution(AVI)

Video S2 shows a liquid metal drop touching a floating silver film in 2 M HCl solution (AVI)

Video S3 shows liquid metal drops running on linear and curved Ag/Au films in 2 M HCl solution (AVI)

Video S4 shows a liquid metal drop contacting a silver film in 1 M HCl solution (AVI)

Video S5 shows a liquid metal drop running uphill at a 22 degrees inclination angle in 2 M HCl solution (AVI)

Video S6 shows liquid metal drops of different sizes running on silver films in 2 M HCl solution (AVI)

■ AUTHOR INFORMATION

Corresponding Author

*E-mail: michael_dickey@ncsu.edu. Tel: (919) 513-0273. Fax: (919) 515-3465

Notes

The authors declare no competing financial interest.

■ ACKNOWLEDGMENTS

This work was supported by NSF CAREER Award number CMMI-0954321 and partially by NSF CMMI-1362284. We thank Nia Christian and Rashed Khan for initial exploratory experiments.

■ REFERENCES

(1) Sammarco, T. S.; Burns, M. A. Thermocapillary Pumping of Discrete Drops in Microfabricated Analysis Devices. *AIChE J.* **1999**, *45*, 350−366.

(2) Pollack, M. G.; Fair, R. B.; Shenderov, A. D. Electrowetting-Based Actuation of Liquid Droplets for Microfluidic Applications. *Appl. Phys. Lett.* **2000**, *77*, 1725.

(3) Darhuber, A. A.; Valentino, J. P.; Davis, J. M.; Troian, S. M.; Wagner, S. Microfluidic Actuation by Modulation of Surface Stresses. *Appl. Phys. Lett.* **2003**, *82*, 657.

(4) Bai, H.; Tian, X.; Zheng, Y.; Ju, J.; Zhao, Y.; Jiang, L. Direction Controlled Driving of Tiny Water Drops on Bioinspired Artificial Spider Silks. *Adv. Mater.* **2010**, *22*, 5521−5525.

(5) Yi, U.-C.; Kim, C.-J. CJ." Soft Printing of Droplets Pre-Metered by Electrowetting. *Sens. Actuators, A* **2004**, *114*, 347−354.

(6) Koch, K.; Dew, B.; Corcoran, T. E.; Przybycien, T. M.; Tilton, R. D.; Garoff, S. Surface Tension Gradient Driven Spreading on Aqueous Mucin Solutions: A Possible Route to Enhanced Pulmonary Drug Delivery. *Mol. Pharmaceutics* **2011**, *8*, 387−394.

(7) Parker, A. R.; Lawrence, C. R. Water Capture by a Desert Beetle. *Nature* **2001**, *414*, 33−34.

(8) Ju, J.; Bai, H.; Zheng, Y.; Zhao, T.; Fang, R.; Jiang, L. A Multi-Structural and Multi-Functional Integrated Fog Collection System in Cactus. *Nat. Commun.* **2012**, *3*, 1247.

(9) Hirokawa, N. Kinesin and Dynein Superfamily Proteins and the Mechanism of Organelle Transport. *Science* **1998**, *279*, 519−526.

(10) Pollard, T. D.; Doberstein, S. K.; Zot, H. G. Myosin-I. *Annu. Rev. Physiol.* **1991**, *53*, 653−682.

(11) Greenspan, H. P. On the Motion of a Small Viscous Droplet That Wets a Surface. *J. Fluid Mech.* **1978**, *84*, 125−143.

(12) Subramanian, R. S. Motion of Drops on Gradient Surfaces. In *Soft Matter Gradient Surfaces: Methods and Applications*; Genzer, J., Ed.; John Wiley & Sons: New York, 2012; pp 407−429.

(13) Brzoska, J. B.; Brochard-Wyart, F.; Rondelez, F. Motions of Droplets on Hydrophobic Model Surfaces Induced by Thermal Gradients. *Langmuir* **1993**, *9*, 2220−2224.

(14) Mettu, S.; Chaudhury, M. K. Motion of Drops on a Surface Induced by Thermal Gradient and Vibration. *Langmuir* **2008**, *24*, 10833−10837.

(15) Darhuber, A. A.; Valentino, J. P.; Troian, S. M.; Wagner, S. Thermocapillary Actuation of Droplets on Chemically Patterned Surfaces by Programmable Microheater Arrays. *J. Microelectromech. Syst.* **2003**, *12*, 873−879.

(16) Pratap, V.; Moumen, N.; Subramanian, R. S. Thermocapillary Motion of a Liquid Drop on a Horizontal Solid Surface. *Langmuir* **2008**, *24*, 5185−5193.

(17) Chaudhury, M. K.; Whitesides, G. M. How to Make Water Run Uphill. *Science* **1992**, *256*, 1539−1541.

(18) Lipowsky, R. Morphological Wetting Transitions at Chemically Structured Surfaces. *Curr. Opin. Colloid Interface Sci.* **2001**, *6*, 40−48.

(19) Daniel, S.; Chaudhury, M. K.; Chen, J. C. Fast Drop Movements Resulting from the Phase Change on a Gradient Surface. *Science* **2001**, *291*, 633−636.

(20) Lugli, F.; Fioravanti, G.; Pattini, D.; Pasquali, L.; Montecchi, M.; Gentili, D.; Murgia, M.; Hemmatian, Z.; Cavallini, M.; Zerbetto, F. And Yet It Moves! Microfluidics Without Channels and Troughs. *Adv. Funct. Mater.* **2013**, *23*, 5543−5549.

(21) Hernández, S. C.; Bennett, C. J. C.; Junkermeier, C. E.; Tsoi, S. D.; Bezares, F. J.; Stine, R.; Robinson, J. T.; Lock, E. H.; Boris, D. R.; Pate, B. D.; et al. Chemical Gradients on Graphene To Drive Droplet Motion. *ACS Nano* **2013**, *7*, 4746−4755.

(22) Subramanian, R. S.; Moumen, N.; McLaughlin, J. B. Motion of a Drop on a Solid Surface Due to a Wettability Gradient. *Langmuir* **2005**, *21*, 11844−11849.

(23) Bain, C. D.; Burnett-Hall, G. D.; Montgomerie, R. R. Rapid Motion of Liquid Drops. *Nature* **1994**, *372*, 414−415.

(24) Dos Santos, F. D.; Ondarçuhu, T. Free-Running Droplets. *Phys. Rev. Lett.* **1995**, *75*, 2972−2975.

(25) Lee, S.-W.; Laibinis, P. E. Directed Movement of Liquids on Patterned Surfaces Using Noncovalent Molecular Adsorption. *J. Am. Chem. Soc.* **2000**, *122*, 5395−5396.

(26) Lee, S.-W.; Kwok, D. Y.; Laibinis, P. E. Chemical Influences on Adsorption-Mediated Self-Propelled Drop Movement. *Phys. Rev. E: Stat. Phys., Plasmas, Fluids, Relat. Interdiscip. Top.* **2002**, *65*, 051602.

(27) Lazar, P.; Riegler, H. Reversible Self-Propelled Droplet Movement: A New Driving Mechanism. *Phys. Rev. Lett.* **2005**, *95*, 136103.

(28) Kumar, G.; Prabhu, K. N. Review of Non-Reactive and Reactive Wetting of Liquids on Surfaces. *Adv. Colloid Interface Sci.* **2007**, *133*, 61−89.

(29) Yao, X.; Bai, H.; Ju, J.; Zhou, D.; Li, J.; Zhang, H.; Yang, B.; Jiang, L. Running Droplet of Interfacial Chemical Reaction Flow. *Soft Matter* **2012**, *8*, 5988−5991.

(30) Shastry, A.; Case, M. J.; Böhringer, K. F. Directing Droplets Using Microstructured Surfaces. *Langmuir* **2006**, *22*, 6161−6167.

(31) Zhang, J.; Han, Y. Shape-Gradient Composite Surfaces: Water Droplets Move Uphill. *Langmuir* **2007**, *23*, 6136−6141.

(32) Khoo, H. S.; Tseng, F.-G. Spontaneous High-Speed Transport of Subnanoliter Water Droplet on Gradient Nanotextured Surfaces. *Appl. Phys. Lett.* **2009**, *95*, 063108.

(33) Liu, C.; Ju, J.; Ma, J.; Zheng, Y.; Jiang, L. Directional Drop Transport Achieved on High-Temperature Anisotropic Wetting Surfaces. *Adv. Mater.* **2014**, *26*, 6086−6091.

(34) Gallardo, B. S.; Gupta, V. K.; Eagerton, F. D.; Jong, L. I.; Craig, V. S.; Shah, R. R.; Abbott, N. L. Electrochemical Principles for Active Control of Liquids on Submillimeter Scales. *Science* **1999**, *283*, 57−60.

(35) Ichimura, K.; Oh, S. K.; Nakagawa, M. Light-Driven Motion of Liquids on a Photoresponsive Surface. *Science* **2000**, *288*, 1624−1626.

(36) Oh, S.-K.; Nakagawa, M.; Ichimura, K. Photocontrol of Liquid Motion on an Azobenzene Monolayer. *J. Mater. Chem.* **2002**, *12*, 2262−2269.

(37) Yamada, R.; Tada, H. Manipulation of Droplets by Dynamically Controlled Wetting Gradients. *Langmuir* **2005**, *21*, 4254−4256.

(38) Florea, L.; Wagner, K.; Wagner, P.; Wallace, G. G.; Benito-Lopez, F.; Officer, D. L.; Diamond, D. Photo-Chemopropulsion - Light-Stimulated Movement of Microdroplets. *Adv. Mater.* **2014**, *26*, 7339−7345.

(39) Prins, M. W. J.; Welters, W. J. J.; Weekamp, J. W. Fluid Control in Multichannel Structures by Electrocapillary Pressure. *Science* **2001**, *291*, 277−280.

(40) Bain, C. D. Motion of Liquids on Surfaces. *ChemPhysChem* **2001**, *2*, 580−582.

(41) Pismen, L. M.; Thiele, U. Asymptotic Theory for a Moving Droplet Driven by a Wettability Gradient. *Phys. Fluids* **2006**, *18*, 042104.

(42) Daniel, S.; Chaudhury, M. K. Rectified Motion of Liquid Drops on Gradient Surfaces Induced by Vibration. *Langmuir* **2002**, *18*, 3404−3407.

(43) Daniel, S.; Sircar, S.; Gliem, J.; Chaudhury, M. K. Ratcheting Motion of Liquid Drops on Gradient Surfaces. *Langmuir* **2004**, *20*, 4085−4092.

(44) Kim, J.; Shen, W.; Latorre, L.; Kim, C.-J. A Micromechanical Switch with Electrostatically Driven Liquid-Metal Droplet. *Sens. Actuators, A* **2002**, *97*−*98*, 672−679.

(45) Latorre, L.; Kim, J.; Lee, J.; de Guzman, P. P.; Lee, H. J.; Nouet, P.; Kim, C. J. Electrostatic Actuation of Microscale Liquid-Metal Droplets. *J. Microelectromech. Syst.* **2002**, *11*, 302−308.

(46) Tang, S.-Y.; Khoshmanesh, K.; Sivan, V.; Petersen, P.; O'Mullane, A. P.; Abbott, D.; Mitchell, A.; Kalantar-zadeh, K. Liquid Metal Enabled Pump. *Proc. Natl. Acad. Sci. U. S. A.* **2014**, *111*, 3304−3309.

(47) Nakata, S.; Komoto, H.; Hayashi, K.; Menzinger, M. Mercury Drop "Attacks" an Oxidant Crystal. *J. Phys. Chem. B* **2000**, *104*, 3589−3593.

(48) Zhang, J.; Yao, Y.; Sheng, L.; Liu, J. Self-Fueled Biomimetic Liquid Metal Mollusk. *Adv. Mater.* **2015**, *27*, 2648−2655.

(49) Kanjanachuchai, S.; Euaruksakul, C. Self-Running Ga Droplets on GaAs (111)A and (111)B Surfaces. *ACS Appl. Mater. Interfaces* **2013**, *5*, 7709−7713.

(50) Hilner, E.; Zakharov, A. A.; Schulte, K.; Kratzer, P.; Andersen, J. N.; Lundgren, E.; Mikkelsen, A. Ordering of the Nanoscale Step Morphology As a Mechanism for Droplet Self-Propulsion. *Nano Lett.* **2009**, *9*, 2710−2714.

(51) Tersoff, J.; Jesson, D. E.; Tang, W. X. Running Droplets of Gallium from Evaporation of Gallium Arsenide. *Science* **2009**, *324*, 236−238.

(52) Tang, W.-X.; Zheng, C.-X.; Zhou, Z.-Y.; Jesson, D. E.; Tersoff, J. Ga Droplet Surface Dynamics during Langmuir Evaporation of GaAs. *IBM J. Res. Dev.* **2011**, *55*, 10:1−10:7.

(53) Wu, J.; Wang, Z. M.; Li, A. Z.; Benamara, M.; Li, S.; Salamo, G. J. Nanoscale Footprints of Self-Running Gallium Droplets on GaAs Surface. *PLoS One* **2011**, *6*, e20765.

(54) Tang, X.; Tang, S.-Y.; Sivan, V.; Zhang, W.; Mitchell, A.; Kalantar-zadeh, K.; Khoshmanesh, K. Photochemically Induced Motion of Liquid Metal Marbles. *Appl. Phys. Lett.* **2013**, *103*, 174104.

(55) Tang, S.-Y.; Sivan, V.; Khoshmanesh, K.; O'Mullane, A. P.; Tang, X.; Gol, B.; Eshtiaghi, N.; Lieder, F.; Petersen, P.; Mitchell, A.; Kalantar-zadeh, K. Electrochemically Induced Actuation of Liquid Metal Marbles. *Nanoscale* **2013**, *5*, 5949−5957.

(56) French, S. J.; Saunders, D. J.; Ingle, G. W. The System Gallium-Indium. *J. Phys. Chem.* **1937**, *42*, 265−274.

(57) Zrnic, D.; Swatik, D. S. On the Resistivity and Surface Tension of the Eutectic Alloy of Gallium and Indium. *J. Less-Common Met.* **1969**, *18*, 67−68.

(58) Koster, J. N.; Derebail, R.; Grötzbach, A. Visualization of Convective Solidification in a Vertical Layer of Eutectic Ga-In Melt. *Appl. Phys. A: Mater. Sci. Process.* **1996**, *64*, 45−54.

(59) Dickey, M. D.; Chiechi, R. C.; Larsen, R. J.; Weiss, E. A.; Weitz, D. A.; Whitesides, G. M. Eutectic Gallium-Indium (EGaIn): A Liquid Metal Alloy for the Formation of Stable Structures in Microchannels at Room Temperature. *Adv. Funct. Mater.* **2008**, *18*, 1097−1104.

(60) Doudrick, K.; Liu, S.; Mutunga, E. M.; Klein, K. L.; Damle, V.; Varanasi, K. K.; Rykaczewski, K. Different Shades of Oxide: From Nanoscale Wetting Mechanisms to Contact Printing of Gallium-Based Liquid Metals. *Langmuir* **2014**, *30*, 6867−6877.

(61) Sheng, L.; Zhang, J.; Liu, J. Diverse Transformations of Liquid Metals Between Different Morphologies. *Adv. Mater.* **2014**, *26*, 6036−6042.

(62) Kramer, R. K.; Boley, J. W.; Stone, H. A.; Weaver, J. C.; Wood, R. J. Effect of Microtextured Surface Topography on the Wetting Behavior of Eutectic Gallium−Indium Alloys. *Langmuir* **2014**, *30*, 533−539.

(63) Glickman, E.; Levenshtein, M.; Budic, L.; Eliaz, N. Interaction of Liquid and Solid Gallium with Thin Silver Films: Synchronized Spreading and Penetration. *Acta Mater.* **2011**, *59*, 914−926.

(64) Benjamin, P.; Weaver, C. The Adhesion of Evaporated Metal Films on Glass. *Proc. R. Soc. London, Ser. A* **1961**, *261*, 516−531.

(65) Mohammed, M. G.; Xenakis, A.; Dickey, M. D. Production of Liquid Metal Spheres by Molding. *Metals* **2014**, *4*, 465−476.

(66) Fosdick, S. E.; Knust, K. N.; Scida, K.; Crooks, R. M. Bipolar Electrochemistry. *Angew. Chem., Int. Ed.* **2013**, *52*, 10438−10456.

(67) Rezai, P.; Salam, S.; Selvaganapathy, P. R.; Gupta, B. P. Transport, Localization and Separation of Caenorhabditis Elegans Using Electrotaxis for Movement Based Behavioral Assays in Drug Discovery. In *14th International Conference on Miniaturized Systems for Chemistry and Life Sciences*; Groningen, The Netherlands, Oct 3−7, 2010 ; Chemical and Biological Microsystems Society: San Diego, CA, 2010; Vol. *1*, pp 160−162.

(68) Xu, J.-X.; Deng, X. Biological Modeling of Complex Chemotaxis Behaviors for C. Elegans under Speed Regulation—a Dynamic Neural Networks Approach. *J. Comput. Neurosci.* **2013**, *35*, 19−37.

(69) Videler, J. J.; Wardle, C. S. Fish Swimming Stride by Stride: Speed Limits and Endurance. *Rev. Fish Biol. Fish.* **1991**, *1*, 23−40.

(70) Kanjanachuchai, S.; Euaruksakul, C. Directions and Breakup of Self-Running In Droplets on Low-Index InP Surfaces. *Cryst. Growth Des.* **2014**, *14*, 830−834.

DOI: 10.1021/acsami.5b06978
ACS Appl. Mater. Interfaces 2015, 7, 23163−23171